



Brittle fracture dynamics with arbitrary paths. II. Dynamic crack branching under general antiplane loading

M. Adda-Bedia*

*Laboratoire de Physique Statistique de l'Ecole Normale Supérieure, 24 rue Lhomond,
F-75231 Paris Cedex 05, France*

Received 12 June 2003; accepted 15 October 2003

Abstract

The dynamic propagation of a bifurcated crack under antiplane loading is considered. The dependence of the stress intensity factor just after branching is given as a function of the stress intensity factor just before branching, the branching angle and the instantaneous velocity of the crack tip. The jump in the dynamic energy release rate due to the branching process is also computed. Similar to the single crack case, a growth criterion for a branched crack is applied. It is based on the equality between the energy flux into each propagating tip and the surface energy which is added as a result of this propagation. It is shown that the minimum speed of the initial single crack which allows branching is equal to $0.39c$, where c is the shear wave speed. At the branching threshold, the corresponding bifurcated cracks start their propagation at a vanishing speed with a branching angle of approximately 40° .

© 2003 Elsevier Ltd. All rights reserved.

Keywords: A. Crack branching and bifurcation; Dynamic fracture; Stress intensity factors; B. Crack mechanics; C. Analytic functions

1. Introduction

In a previous paper (Adda-Bedia and Arias, 2003), a method for determining the elastodynamic stress fields associated with the propagation of antiplane kinked or branched cracks was developed. As a first illustration, the case of a semi-infinite antiplane straight crack, initially propagating at a given time-dependent velocity, that changes instantaneously both its direction and its speed of propagation was considered. The aim of the

* Tel.: +33-1-44-32-25-26; fax: +33-1-44-32-34-33.

E-mail address: adda@lps.ens.fr (M. Adda-Bedia).

present paper is to apply this method to the case of an initially propagating antiplane crack that branches into two cracks that merge symmetrically. The explicit dependence of the stress intensity factor just after branching is given as a function of the stress intensity factor just before branching, the branching angle and the instantaneous velocity of the crack tip.

A growth criterion for a branched crack must be based on the equality between the energy flux into the two propagating tips and the surface energy which is added as a result of this propagation. Eshelby proposed this approach (Eshelby, 1970; Rice et al., 1994) posing the question how large must be the single crack speed so that there will be enough energy available to form two slow cracks instead of the single fast one. Using the exact solution, the jump in the dynamic energy release rate due to the branching process is computed. It is shown that the minimum speed of the initial single crack which allows branching is equal to $0.39c$, where c is the shear wave speed. The corresponding bifurcated cracks start their propagation at a vanishing speed with a branching angle of 39.6° .

The paper is organized as follows. The next section summarizes the approach to the branched crack dynamics under mode III loading. The corresponding model problem is presented, and the self-similar solution that it admits is derived. The analysis of this section is similar to the dynamical kinked crack problem, and a detailed discussion can be found in Adda-Bedia and Arias (2003). In Section 3, the dynamic crack branching problem is completely solved. The self-similar solution of the corresponding problem is given by an integral representation, which is a convolution between a known kernel and a harmonic function, which is determined by a different method than that used for the kinked crack case (Adda-Bedia and Arias, 2003). It is shown that the problem can be reduced to the determination of a real function that satisfies a simple integral equation. Once the integral equation is solved, the stress intensity factor just after branching is computed a posteriori using an additional condition. In the last section, the stress intensity factor just after branching and the jump in the dynamic energy release rate due to the branching process are given for arbitrary angles and velocities. Finally, following Eshelby's approach (Eshelby, 1970; Rice et al., 1994), the growth criterion for a branched crack is applied, and the minimum speed of the initial single crack which can allow branching is computed.

2. The dynamical branched crack under mode III loading

Consider an elastic body which contains a branched crack but which is otherwise unbounded (see Fig. 1). Introduce a cylindrical coordinate system (r, θ, z) so that the z -axis lies along the crack edge. Suppose that the material is subjected to a loading which produces a state of antiplane shear deformation in the body. Thus the only nonzero component of displacement is the z -component $u_z(r, \theta, t) \equiv w(r, \theta, t)$, which is independent of z .

The scenario of crack branching is decomposed as follows. A semi-infinite straight crack that propagates at a speed $v(t)$ for $t < -\tau$, with $\tau \rightarrow 0^+$, suddenly stops at $t = -\tau$. At $t \rightarrow 0^+$, the crack branches locally with a branching angle equal to $\lambda\pi$,

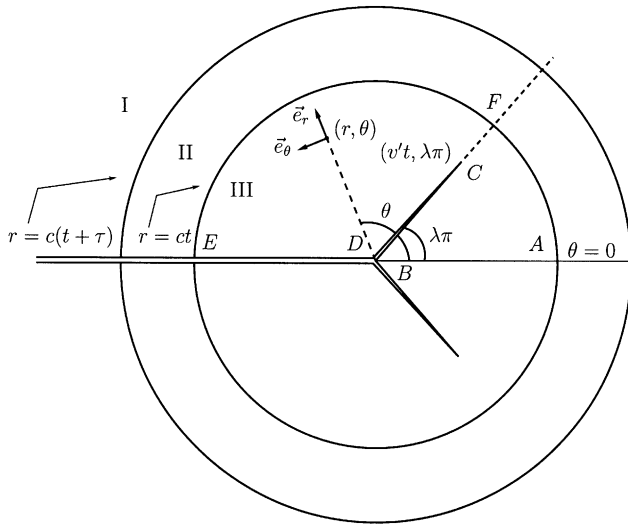


Fig. 1. A half-plane crack that propagates at a speed v for $t < -\tau$ suddenly stops at $t = -\tau$. For $t > 0$, the new branches propagate straightly from the position $r = 0$ at a velocity v' , following the directions $\pm\lambda\pi$. The orthonormal basis $(\vec{e}_r, \vec{e}_\theta, \vec{e}_z)$ corresponding to the cylindrical coordinate system (r, θ, z) is shown. The cylindrical waves originated at the crack's arrest ($r = c(t + \tau)$) and at the start of branches propagation ($r = ct$) divide the material into three regions. In the region labelled I, the stress field comes only from the dynamical straight crack propagation, since the effects of the crack's arrest and the crack's branching are not experienced there. The region II is influenced by the crack arrest only, thus the stress field there is a static one (Eshelby, 1969; Freund, 1990). It is only the region III that is influenced by the crack's branching. Thus, one has to solve the branched crack problem only in this latter region.

with $0 < \lambda < 1$. For $t > 0$, the new branches propagate straightly at a velocity $v'(t)$, following the new directions $\pm\lambda\pi$. The magnitude of the crack speed v and v' are restricted by $0 < v < c$ and $0 < v' < c$, where c denotes the shear wave speed. The mode III dynamic stress intensity factor, $K(t)$, of the straight crack prior to branching is related to the rest stress intensity factor, $K_0(t)$, of the same configuration by (Eshelby, 1969; Kostrov, 1966; Freund, 1990)

$$K(t) = k(v)K_0(t), \tag{1}$$

where $k(v)$ is a universal function of the instantaneous crack tip speed given by

$$k(v) = \sqrt{1 - v/c}. \tag{2}$$

According to the latter description of crack branching, the dynamic stress intensity factor, K' , just after branching should be defined by

$$K'(\lambda, v, v', c, \dots) = \lim_{\tau \rightarrow 0^+} \lim_{t \rightarrow 0^+} \lim_{(r-v't) \rightarrow 0^+} \sqrt{2\pi(r - v't)} \sigma_{\theta z}(r, \lambda\pi, t). \tag{3}$$

When the initial crack stops, a static stress distribution is restored behind a wave front that propagates from the crack tip at the shear wave speed (Eshelby, 1969; Freund, 1990), (see Fig. 1). Moreover, in the limit $t \rightarrow 0^+$, the lengths of the branched

parts of the crack are vanishingly small, so that the breaking process after branching occurs in the region determined by the square root singular stress intensity factor field of the semi-infinite straight crack. Therefore, the branching problem consists in two symmetric branches reminiscent from a preexisting stationary straight crack, that start to propagate at time $t = 0^+$, in the directions $\pm\lambda\pi$, with a velocity v' , under the action of a time-independent loading, $\sigma_{\theta z}^s(r, \theta)$, given by (Adda-Bedia and Arias, 2003)

$$\sigma_{\theta z}^s(r, \theta) = \frac{K_0}{\sqrt{2\pi r}} \cos \frac{\theta}{2}, \quad (4)$$

where K_0 is the rest stress intensity factor of the crack tip prior to branching. A straightforward consequence of these dimensional arguments is that the stress intensity factor just after branching must be written as (Adda-Bedia and Arias, 2003)

$$K' = k(v')H_{33}(\lambda, v'/c)K_0, \quad (5)$$

where H_{33} is an unknown dimensionless function of the branching angle $\lambda\pi$ and of the crack tip speed v' only. The function H_{33} is universal in the sense that it depends on neither the loading configuration nor on the geometry of the body. Effectively, in the limits $t \rightarrow 0^+$ and $\tau \rightarrow 0^+$ that we consider, the dynamic branching problem does not involve radiation effects. So it is always equivalent to a crack propagating in an unbounded body. On the other hand, due to the absence of intrinsic time or length scales in linear elasticity theory, this problem becomes of general purpose, because it is not necessary for the crack and for the branches to be straight. H_{33} does not depend on the local curvature of the crack prior to or after branching (Adda-Bedia and Arias, 2003).

2.1. The model problem of dynamic crack branching

The process of crack advance in the situation depicted in Fig. 1 can be viewed as follows. For $t < 0$, it is assumed that the crack is at rest and that the material is loaded according to Eq. (4). As the crack advances for $t > 0$, the component of displacement $w(r, \theta, t)$ satisfies the wave equation

$$\frac{1}{r} \frac{\partial}{\partial r} \left(r \frac{\partial w}{\partial r} \right) + \frac{1}{r^2} \frac{\partial^2 w}{\partial \theta^2} = \frac{1}{c^2} \frac{\partial^2 w}{\partial t^2} \quad (6)$$

with boundary conditions on the displacement field $w(r, \theta, t)$, for $r \leq ct$, given by

$$\sigma_{\theta z}(r, \pi, t) = 0, \quad (7)$$

$$w(r, 0, t) = 0, \quad (8)$$

$$\sigma_{\theta z}(r < v't, \lambda\pi \pm \varepsilon, t) = 0, \quad (9)$$

$$w(ct, \theta, t) = \frac{2K_0}{\mu} \sqrt{\frac{ct}{2\pi}} \sin \frac{\theta}{2}. \quad (10)$$

Here (and elsewhere), ε is a vanishingly small positive constant, μ is the shear modulus, and

$$\sigma_{\theta z} = \frac{\mu}{r} \frac{\partial w}{\partial \theta}.$$

Condition (8) follows from the symmetry property of $w(r, \theta, t)$ with respect to reflection in the plane $\theta=0$. Condition (9) is a consequence of the continuity of the displacement field $w(r, \theta, t)$ at the wave front $r = ct$. Moreover, the dynamic jump condition across the wave front $r = ct$ is given by (Dempsey et al., 1982)

$$[\sigma_{rz}]_{r=ct} + \frac{\mu}{c} \left[\frac{\partial w}{\partial t} \right]_{r=ct} = 0, \tag{11}$$

where

$$\sigma_{rz} = \mu \frac{\partial w}{\partial r}.$$

The Williams expansion (Williams, 1952) imposes that the singularity of $\sigma_{\theta z}(r, \theta, t)$ in the vicinity of the edge points B and D should be given by

$$\sigma_{\theta z}(r, \theta, t) \sim r^p \quad \text{as } r \rightarrow 0, \tag{12}$$

where

$$p = \begin{cases} \frac{\lambda}{1-\lambda} & \text{for } \lambda\pi < \theta < \pi, \\ -1 + \frac{1}{2\lambda} & \text{for } 0 < \theta < \lambda\pi. \end{cases} \tag{13}$$

The asymptotic behavior of the stress field near the propagating crack tip is given by (Freund, 1990)

$$\sigma_{\theta z}(r, \lambda\pi \pm \varepsilon, t) = \left[\frac{K'}{\sqrt{2\pi(r-v't)}} + O(\sqrt{r-v't}) \right] H(r-v't) \tag{14}$$

as $r \rightarrow v't$,

where H is the heaviside function.

2.2. Self-similar analysis

Except the stress intensity factor scale introduced by the boundary condition (10), there is neither a characteristic length nor a characteristic time against which the independent variables r and t can be scaled. Therefore, the displacement field takes the following self-similar form (Adda-Bedia and Arias, 2003):

$$w(r, \theta, t) = \frac{K_0}{\mu} \sqrt{\frac{r}{2\pi}} \left[2 \sin \frac{\theta}{2} + W(s, \theta) \right], \tag{15}$$

where

$$s \equiv \cosh^{-1} \left(\frac{ct}{r} \right), \quad s \geq 0 \tag{16}$$

and W is a dimensionless function of its arguments (Miles, 1960; Dempsey et al., 1982; Broberg, 1999). Equivalently, the stress field takes the following form:

$$\sigma_{\theta z}(r, \theta, t) = \frac{K_0}{\sqrt{2\pi r}} \left[\cos \frac{\theta}{2} + S(s, \theta) \right] \tag{17}$$

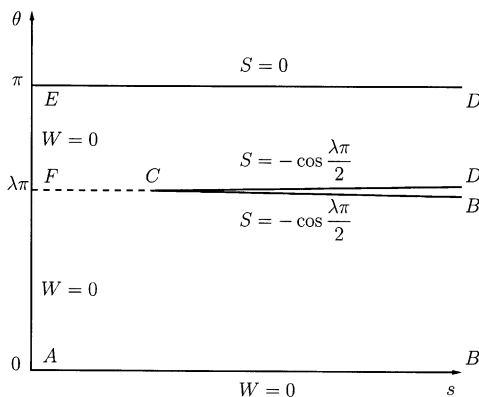


Fig. 2. The (s, θ) -plane, with $s \geq 0$ and $0 \leq \theta \leq \pi$, that maps the region III of (r, θ, t) -space, corresponding to $r \leq ct$, $0 \leq \theta \leq \pi$, and $t > 0$ (see Fig. 1).

with

$$S(s, \theta) = \frac{\partial W}{\partial \theta}(s, \theta). \tag{18}$$

In Fig. 2, the transformation from the coordinates system (r, θ, t) to the (s, θ) -plane is shown. Taking into account the explicit dependence of s on r and t , one finds that W satisfies the partial differential equation

$$\frac{\partial^2 W}{\partial s^2} - \coth s \frac{\partial W}{\partial s} + \frac{\partial^2 W}{\partial \theta^2} + \frac{1}{4} W = 0. \tag{19}$$

The singularity of the stress field in the vicinity the edge points B and D , as given by Eq. (12), imposes the behavior to the function $S(s, \theta)$

$$S(s, \theta) = -\cos \frac{\theta}{2} + O\left(\exp - \left(p + \frac{1}{2}\right) s\right) \quad \text{as } s \rightarrow +\infty, \tag{20}$$

On the other hand, the asymptotic behavior near the crack tip (14) imposes the following asymptotic behavior in the (s, θ) -plane:

$$S(s, \lambda\pi \pm \varepsilon) = -\cos \frac{\lambda\pi}{2} + \left[\frac{K'}{K_0} \frac{\sqrt{\coth b}}{\sqrt{b-s}} + O\left(\sqrt{b-s}\right) \right] H(b-s) \tag{21}$$

as $s \rightarrow b$,

where

$$b \equiv \cosh^{-1}(c/v'). \tag{22}$$

The boundary conditions (7)–(10) are easily transformed into conditions on W and S . They are given by

$$S(s, \pi) = 0, \tag{23}$$

$$W(s, 0) = 0, \tag{24}$$

$$S(s > b, \lambda\pi \pm \varepsilon) = -\cos \frac{\lambda\pi}{2}, \tag{25}$$

$$W(0, \theta) = 0. \tag{26}$$

Once the displacement field $w(r, \theta, t)$ is written under the form (15), the jump condition (11) across the cylindrical wave front $s = 0$, corresponding to $r = ct$, is automatically satisfied.

3. Solution of the dynamic crack branching problem

In Adda-Bedia and Arias (2003), it has been shown that Eq. (19) admits solutions of the form

$$W(s, \theta) = \frac{2}{\pi} \int_0^s \sqrt{\cosh s - \cosh s'} \Phi(s', \theta) ds', \tag{27}$$

where $\Phi(s, \theta)$ is an unknown function that satisfies the harmonic equation

$$\left[\frac{\partial^2}{\partial s^2} + \frac{\partial^2}{\partial \theta^2} \right] \Phi(s, \theta) = 0, \tag{28}$$

and the additional boundary condition

$$\left[\frac{\partial}{\partial s} \Phi(s, \theta) \right]_{s=0} = 0. \tag{29}$$

Note that once the displacement function $W(s, \theta)$ is written in the form (27), the boundary condition (26) at the cylindrical wave front $s = 0$ is automatically satisfied. Eq. (28) implies that the function $\Phi(s, \theta)$ is readily given by the real part of a complex function $F(\gamma = s + i\theta)$, which is holomorphic inside the contour $DCBAED$ (see Fig. 2):

$$\Phi(s, \theta) = \text{Re}[F(\gamma)] \equiv \frac{1}{2}[F(\gamma) + \overline{F(\gamma)}], \quad \gamma = s + i\theta. \tag{30}$$

Using Eq. (30) and Cauchy relations for holomorphic functions, the function $S(s, \theta)$ can thus be written in the form

$$S(s, \theta) = \frac{1}{\pi} \sqrt{\cosh s - 1} \text{Im}[F(i\theta)] - \int_0^s \frac{\sinh s' \text{Im}[F(s' + i\theta)]}{\sqrt{\cosh s - \cosh s'}} \frac{ds'}{\pi}. \tag{31}$$

Condition (20) imposes that the stress function $S(s, \theta)$ is not diverging at $s \rightarrow +\infty$. This imposes that

$$\text{Im}[F(i\theta)] = 0. \tag{32}$$

Moreover, Eq. (32) is a sufficient condition for satisfying the boundary condition (29). Therefore, Eq. (31) is reduced to

$$S(s, \theta) = - \int_0^s \frac{\sinh s' \text{Im}[F(s' + i\theta)]}{\sqrt{\cosh s - \cosh s'}} \frac{ds'}{\pi}. \tag{33}$$

Using Eq. (33), expansion (20) in the vicinity of the wedge points B and D are recovered if the function F satisfies the following behavior:

$$\text{Im}[F(\gamma)] \rightarrow \sqrt{2} \exp \left[-\frac{s}{2} \right] \cos \frac{\theta}{2} \quad \text{as } \gamma \rightarrow \infty. \tag{34}$$

The asymptotic behavior near the crack tip embodied in Eq. (21) imposes a specific behavior of $F(\gamma)$ in the neighborhood of the corresponding point $\gamma_C \equiv b + i\lambda\pi$. It can be shown that $F(\gamma)$ behaves as (Adda-Bedia and Arias, 2003)

$$F(\gamma) = \frac{ia}{\gamma - \gamma_C} + O((\gamma - \gamma_C)^0) \quad \text{as } \gamma \rightarrow \gamma_C \equiv b + i\lambda\pi, \tag{35}$$

where a is a real constant that satisfies

$$a = \frac{\sqrt{\cosh b} K'}{\sinh b K_0}. \tag{36}$$

Thus, the function F has a simple pole at $\gamma = \gamma_C$. The boundary conditions (23), (24) on S imply that $F(\gamma)$ must satisfy

$$\text{Im}[F(s + i\pi)] = 0, \tag{37}$$

$$\text{Re}[F(s)] = 0. \tag{38}$$

Finally, the transformation of the boundary condition (25) on S onto a condition satisfied by F leads to (Adda-Bedia and Arias, 2003)

$$\begin{aligned} &\sqrt{\cosh s - \cosh b} \text{Im}[F(s + i(\lambda\pi \pm \varepsilon))] \\ &= \cos \frac{\lambda\pi}{2} - \int_0^b \frac{\sqrt{\cosh b - \cosh s'}}{\cosh s - \cosh s'} \sinh s' \text{Im}[F(s' + i\lambda\pi)] \frac{ds'}{\pi}, \quad s > b. \end{aligned} \tag{39}$$

The holomorphic function $F(\gamma)$ is uniquely determined by conditions (32), (34), (35), (37)–(39). On the other hand, using Eq. (36), the stress intensity factor just after branching, K' , is determined once the real constant a is fixed.

In the following, the dynamic crack branching problem will be solved using a different method than the one for the dynamic kinked crack problem (Adda-Bedia and Arias, 2003). For the present case, it is possible to get a suitable representation of the function $F(\gamma)$ without mapping it into a complex half-plane (Adda-Bedia and Arias, 2003). An intermediate solution of $F(\gamma)$, which satisfies the conditions (32), (35), (37), (38), is given by

$$F(\gamma) = 2a \cosh(b/2) [F_1(\gamma) + F_2(\gamma)], \tag{40}$$

where $F_1(\gamma)$ and $F_2(\gamma)$ are holomorphic functions inside the contour $DCBAED$, given by

$$F_1(\gamma) = i \left[\frac{\sinh((\gamma - i\lambda\pi)/2)}{\cosh(\gamma - i\lambda\pi) - \cosh(b)} + \frac{\sinh((\gamma + i\lambda\pi)/2)}{\cosh(\gamma + i\lambda\pi) - \cosh(b)} \right], \tag{41}$$

$$F_2(\gamma) = i \int_b^\infty \left[\frac{\sinh((\gamma - i\lambda\pi)/2)}{\cosh(\gamma - i\lambda\pi) - \cosh(t)} + \frac{\sinh((\gamma + i\lambda\pi)/2)}{\cosh(\gamma + i\lambda\pi) - \cosh(t)} \right] f(t) dt, \tag{42}$$

with $f(t)$ a real continuous function defined for $t > b$. Written in the forms (41), (42), the functions $F_1(\gamma)$ and $F_2(\gamma)$, and consequently $F(\gamma)$, satisfy automatically the conditions (32), (37), (38). Also, condition (35) is automatically satisfied by $F(\gamma)$, through $F_1(\gamma)$. Finally, notice that $F_2(\gamma)$, as given by Eq. (42), is the most general representation of a holomorphic function that satisfy the conditions (32), (37), (38).

Therefore, the complete determination of the function $F(\gamma)$ is now reduced to finding the real function f and the real constant a . They are fixed by the integral equation (39) satisfied by F (or f), combined with the additional condition (34), which can be rewritten as

$$2\sqrt{2} a \cos(\lambda\pi/2) \cosh(b/2) \left[1 + \int_b^\infty f(t) dt \right] = 1. \tag{43}$$

Using Eqs. (36) and (43), the stress intensity factor just after branching, K' , is then given by

$$\frac{K'}{K_0} \equiv k(v') H_{33}(\lambda, v'/c) = \frac{k(v')}{2 \cos(\lambda\pi/2) [1 + \int_b^\infty f(t) dt]}. \tag{44}$$

The function f must satisfy the integral equation (39), which can be simplified to (see Appendix A)

$$f(s) = A(s, b) + \int_b^\infty A(s, u) f(u) du, \quad s > b, \tag{45}$$

$$A(s, u) = \frac{1}{\pi} \frac{\cosh(s/2)}{\cosh(u/2)} \operatorname{Im} \left[\frac{\sinh(u - 2i\lambda\pi)}{\cosh(s) - \cosh(u - 2i\lambda\pi)} \right]. \tag{46}$$

Note that Eqs. (45) and (46) do not involve the real constant a . Therefore, the latter integral equation can be solved independently of the value of the constant a . Once the function f is determined, the stress intensity factor just after branching is computed *a posteriori*, by using Eq. (44).

A complete analytical solution of the integral equation (45) cannot be derived in the general case. However, for the special case $\lambda = 1/2$, it is straightforward to show that $A(s, u) = 0$. Therefore, the solution of Eq. (45) is readily given by $f(s) = 0$, and Eq. (44) yields

$$H_{33}(1/2, v'/c) = \frac{1}{\sqrt{2}}. \tag{47}$$

For the general case, the numerical resolution of integral equation (45) can be done without difficulty. In Fig. 3, examples of solutions are shown for some values of λ and v' . In Fig. 4, the function $H_{33}(\lambda, v'/c)$ is plotted as a function of the branching angle and for some values of the speed of the crack branches. Note that in Fig. 4, the interval $1/2 \leq \lambda \leq 1$ has not been considered, because it is not pertinent for the subsequent discussion.

4. Results and discussion

Using a method developed in Adda-Bedia and Arias (2003), the elastodynamic stress fields associated with the propagation of antiplane branched cracks have been determined. Within this approach, the dynamic stress intensity factor just after branching, as given by Eq. (5), is computed as a function of the stress intensity factor just before branching, the branching angle and the instantaneous velocity of the crack tip. The corresponding results are summarized in Fig. 4. First, it is shown that $H_{33}(0, v'/c) = 1/\sqrt{2}$,

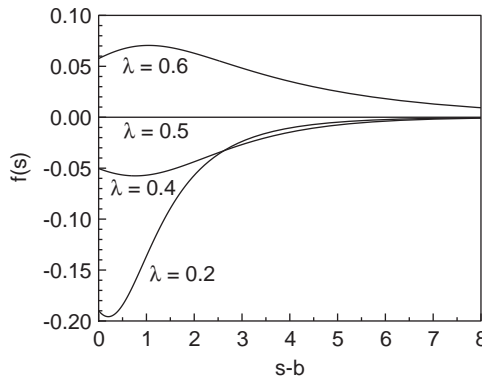


Fig. 3. Plot of the function $f(s)$, solution of Eq. (45), for some values of the branching angle and for $v'/c = 0.2$.

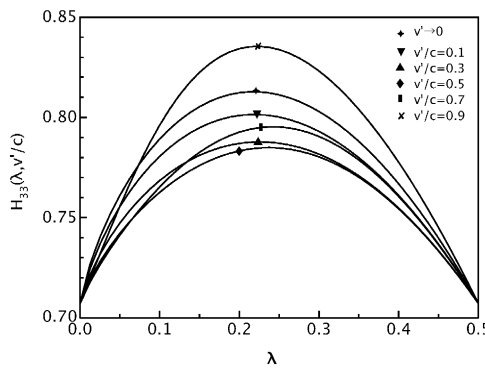


Fig. 4. Plot of the function H_{33} as a function of the branching angle and for some values of the crack tip speed just after branching. Note that $K'/K_0 = \sqrt{1 - v'/c} H_{33}(\lambda, v'/c)$, where K' is the dynamic stress intensity factor just after branching, and K_0 is the rest stress intensity factor just before branching. Note that for $\lambda \rightarrow 0$, H_{33} coincides exactly with the corresponding elastostatic result given by Eq. (48).

independently of v' . For a given branches velocity, H_{33} increases with λ , attains a maximum at a given branching angle that depends on v' , and decreases again with λ , by satisfying $H_{33}(1/2, v'/c) = 1/\sqrt{2}$ and $H_{33}(1, v'/c) = 0$. However, the principal result of Fig. 4 concerns the dynamic stress intensity factor just after branching for a vanishingly small velocity. The latter quantity coincides exactly with the stress intensity factor just after branching computed by using an elastostatic approach (Smith, 1968),

$$H_{33}(\lambda, v' \rightarrow 0) = \frac{1}{\sqrt{2}} \left(\frac{1 - \lambda}{\lambda} \right)^{\lambda/2}. \tag{48}$$

This result differs from the previous one dealing with the kinked crack configuration (Adda-Bedia and Arias, 2003), where the dynamic stress intensity factor just after kinking for a vanishingly small velocity was found to be slightly different from the

corresponding elastostatic solution. This difference may be due to numerical errors induced by the method used in Adda-Bedia and Arias (2003) for computing the dynamic stress intensity factor just after kinking. Indeed, the present approach, as given in Section 3 and in Appendix A, is more elaborated than in Adda-Bedia and Arias (2003). The representation of the function $F(\gamma)$, as given by Eqs. (40)–(42) allowed analytical computations without mapping the function $F(\gamma)$ into a complex half-plane. As a consequence, the resolution of the numerical problem, as given by Eqs. (45) and (46), has been straightforward. Applying the same approach for the kinked crack case would be necessary for validating the behavior of the dynamic stress intensity factor just after kinking, as a function of the kinking angle and of the velocity just after kinking. Unfortunately, an equivalent representation of the corresponding function $F(\gamma)$ for the kinked crack case is not available yet.

4.1. Dynamic branching instability

Eshelby (1970) posed the question how large must be the single crack speed so that there will be enough energy available to form two slow cracks instead of the single fast one. The simplest branched configuration that Eshelby analyzed is the limiting case where the branches subtend a vanishingly small angle and both prolong the original crack plane. In this case, Eshelby reported $v=0.6c$ and $v' \rightarrow 0$ as the minimum speeds which could allow branching or surface roughening (Eshelby, 1970). However, since no solution was available for two branches with an arbitrary angle between them and propagating at arbitrary velocities, this result has been considered as a rough estimate.

The dynamic energy release rate is a quantity associated to a single moving crack tip. It is defined as the rate of mechanical energy flow out of the body and into the crack tip per unit crack advance. For the single moving crack before branching, it is given by (Freund, 1990)

$$G = \frac{K^2}{2\mu\sqrt{1-v^2/c^2}} = \frac{1}{2\mu} g(v)K_0^2, \quad (49)$$

where K_0 is the rest stress intensity factor, and

$$g(v) = \sqrt{\frac{1-v/c}{1+v/c}}. \quad (50)$$

The function $g(v)$ does not depend on the details of the applied loading or the configuration of the body being analyzed. It depends on the local instantaneous speed of the crack tip and on the properties of the material only. Due to the symmetry of the branching configuration, the energy release rate just after branching G' of each crack tip is given by

$$G' = \frac{K'^2}{2\mu\sqrt{1-v'^2/c^2}} = \frac{1}{2\mu} g(v')H_{33}^2(\lambda, v'/c)K_0^2. \quad (51)$$

In Fig. 5, the energy release rate just after branching G' is plotted as a function of the branching angle and for some values of the velocity just after branching. It is

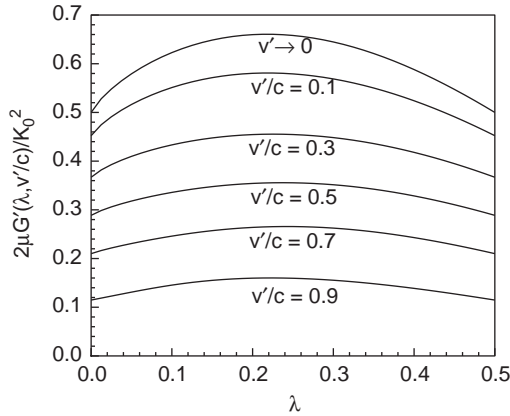


Fig. 5. Plot of the energy release rate just after branching G' , scaled by $K_0^2/(2\mu)$, as a function of the branching angle and for some values of the crack tip speed just after branching.

shown that for a constant branching angle, G' is a decreasing function of v' . Therefore, the energy release rate just after branching is maximized when the branches start to propagate quasi-statically ($v' \rightarrow 0$). Moreover, G' always displays a maximum at a given branching angle that depends on the branches velocity v' .

According to the Generalized Griffith’s criterion (Griffith, 1920), a crack must grow in such a way that its energy release rate is equal to the dynamic fracture energy of the material, Γ , which is assumed to be a property of the material and whose value may depend on the instantaneous crack tip speed. This growth criterion should be applied for each crack tip before and after branching. At the onset of branching, the conditions

$$G \equiv \Gamma(v) \quad \text{and} \quad G' \equiv \Gamma(v'), \tag{52}$$

should be satisfied. Therefore, the growth criterion introduces an intrinsic relationship between the energy release rates just before and just after branching, which reads

$$G' = \frac{\Gamma(v')}{\Gamma(v)} G. \tag{53}$$

Eq. (53) is a necessary condition for the existence of a branching configuration. Otherwise, the single crack tip propagation should be maintained. Moreover, condition (53) shows that if a branching instability occurs, it is universal in the sense that it does not depend either on the loading configuration or on the geometry of the body. The branching thresholds depend on the properties of the material only. In the case of a constant fracture energy, Eq. (53) reduces to

$$g(v) = g(v')H_{33}^2(\lambda, v'/c). \tag{54}$$

Eq. (50) shows that $g(v)$ is a decreasing function of the velocity, which satisfies $g(0) = 1$, and $g(c) = 0$. Moreover, Fig. 5 shows that the right-hand side of Eq. (54) displays a maximum, whose value is smaller than unity. Therefore, branched solutions exist only if the velocity v exceeds a critical velocity v_c . This threshold is given by the

least velocity v for which Eq. (54) admits a solution. This solution corresponds to a branched configuration with a speed $v'_c \rightarrow 0$, and a branching angle of 39.6° ($\lambda_c=0.22$), given by the maximum of $H_{33}(\lambda, 0)$. Using Eq. (54), one finds that the corresponding critical speed of the single crack tip speed before branching is given by $v_c = 0.39c$.

The thresholds of the branching instability given by ($v'_c \rightarrow 0, \lambda_c=0.22, v_c=0.39c$) have to be compared to the ones reported by Eshelby (1970), ($v'_c \rightarrow 0, \lambda_c \rightarrow 0, v_c=0.6c$). The assumptions of zero branching angle and vanishing branches velocity were necessary, as no solution was available for two branches with an arbitrary angle between them and propagating at an arbitrary speed. The present exact computations confirm that the resultant zero velocity after branching is the least velocity for which a branched configuration exists. Consequently, the critical branching angle, which is computed directly from the elastostatic solution, is given by the maximum of $H_{33}(\lambda, 0)$. Therefore, the resultant critical velocity of the initial single crack is smaller than the one computed from the zero branching angle assumption.

Finally, the critical speed for branching, $v_c=0.39c$, agrees with the one deduced from numerical simulations using a phase field model of brittle fracture under antiplane loading (Lobkovsky and Karma, 2003). However, since dynamic fracture experiments are often performed under inplane situations, a theoretical study of this case is still lacking. Although the resolution of a branched configuration of a dynamical crack under inplane loading seems difficult to perform, the analogy with the mode III loading suggests that a quasistatic approach would be sufficient, or at least a good approximation, for the determination of the branching instability thresholds.

Acknowledgements

I wish to thank R. Arias, M. Ben Amar and J.R. Rice for enlightening discussions. Laboratoire de Physique Statistique de l'Ecole Normale Supérieure is associated with CNRS (UMR 8550) and with Universities Paris VI and Paris VII.

Appendix A

In the following, we focus on the transformation of the integral equation (39) into Eq. (45). Using the representations (41), (42), it is shown that

$$\text{Im}[F(s + i\lambda\pi)] = 2a \cosh(b/2) \left[I(s, b) + \int_b^\infty I(s, t) f(t) dt \right], \tag{A.1}$$

$$I(s, t) = \text{Re} \left[\frac{\sinh(s/2)}{\cosh(s) - \cosh(t)} + \frac{\sinh((s + 2i\lambda\pi)/2)}{\cosh(s + 2i\lambda\pi) - \cosh(t)} \right]. \tag{A.2}$$

Eq. (A.2) can be easily transformed into

$$I(s, t) = \frac{\sinh(s/2)}{\cosh(s) - \cosh(t)} + \frac{\sinh(s/2)}{\cosh(t/2)} \text{Re} \left[\frac{\cosh((t - 2i\lambda\pi)/2)}{\cosh(s) - \cosh(t - 2i\lambda\pi)} \right]. \tag{A.3}$$

Using Eqs. (A.1) and (A.3), the integration over s' in Eq. (39) can be computed analytically. After some algebraic manipulation and using Eq. (43), an integral equation satisfied by the real function f is deduced. It is given by

$$\int_b^\infty \frac{\sqrt{\cosh(t) - \cosh(b)}}{\cosh(t) - \cosh(s)} f(t) \sinh(t/2) dt = H(s, b) + \int_b^\infty H(s, t) f(t) dt, \quad (\text{A.4})$$

$$H(s, t) = \text{Re} \left[\frac{\sinh(t - 2i\lambda\pi)}{2 \cosh(t/2)} \frac{\sqrt{\cosh(t - 2i\lambda\pi) - \cosh(b)}}{\cosh(s) - \cosh(t - 2i\lambda\pi)} \right], \quad (\text{A.5})$$

where the integral in the left-hand side of Eq. (A.4) must be taken in the sense of Cauchy principal value. One can write Eq. (A.4) differently by noticing that it is in the form of a Hilbert singular integral equation. Thus, one can invert it to obtain (Muskhelishvili, 1953)

$$f(s) = A(s, b) + \int_b^\infty A(s, u) f(u) du, \quad s > b, \quad (\text{A.6})$$

$$A(s, u) = -2 \cosh(s/2) \int_b^\infty \frac{H(t, u) \sinh(t)}{\sqrt{\cosh(t) - \cosh(b)} (\cosh(t) - \cosh(s))} \frac{dt}{\pi^2}. \quad (\text{A.7})$$

Using Eq. (A.5), one can compute analytically the integration over the variable t in Eq. (A.7). The result leads to Eq. (46).

References

- Adda-Bedia, M., Arias, R., 2003. Brittle fracture dynamics with arbitrary paths-I. Dynamic crack kinking under general antiplane loading. *J. Mech. Phys. Solids* 51, 1287–1304.
- Broberg, K.B., 1999. *Cracks and Fracture*. Academic Press, London.
- Dempsey, J.P., Kuo, M.K., Achenbach, J.D., 1982. Mode III kinking under stress wave loading. *Wave Motion* 4, 181–190.
- Eshelby, J.D., 1969. The elastic field of a crack extending nonuniformly under general antiplane loading. *J. Mech. Phys. Solids* 17, 177–199.
- Eshelby, J.D., 1970. Energy relations and the energy-momentum tensor in continuum mechanics. In: Kanninen, M.F., Adler, W.F., Rosenfield, A.R., Jaffee, R.I. (Eds.), *Inelastic Behaviour of Solids*. McGraw-Hill, New York, pp. 77–115.
- Freund, L.B., 1990. *Dynamic Fracture Mechanics*. Cambridge University Press, New York.
- Griffith, A.A., 1920. The phenomenon of rupture and flow in solids. *Philos. Trans. R. Soc. (London)* A 221, 163–198.
- Kostrov, B.V., 1966. Unsteady propagation of longitudinal shear cracks. *Appl. Math. Mech.* 30, 1241–1248.
- Lobkovsky, A.E., Karma, A., 2003. Unsteady Crack Motion and Branching in a Phase-Field Model of Brittle Fracture, Preprint.
- Miles, J.W., 1960. Homogeneous solutions in elastic wave propagation. *Q. Appl. Math.* 18, 37–59.
- Muskhelishvili, N.I., 1953. *Singular Integral Equations*. Noordhoff, Groningen.
- Rice, J.R., Ben-Zion, Y., Kim, K.S., 1994. Three-dimensional perturbation solution for a dynamic planar crack moving unsteadily in a model elastic solid. *J. Mech. Phys. Solids* 42, 813–843.
- Smith, E., 1968. Crack bifurcation in brittle solids. *J. Mech. Phys. Solids* 16, 329–336.
- Williams, M.L., 1952. Stress singularities resulting from various boundary conditions in angular corners of plates in extension. *J. Appl. Mech.* 19, 526–528.